Recharge Assessment as Influenced by Floodwater Spreading in a Dry Region

Mojtaba Pakparar[1]*

1- Associate Professor, Soil Conservation & Watershed Management Dept., Fars Research & Education Center for Agriculture & Natural Resources, AREEO, Shiraz, Iran*

Abstract

Water scarcity due to climate change and a growing water demand in different consumption sectors is a major environmental crisis that drives arable lands to the state of degradation, especially in dry regions. Artificial recharge of groundwater (ARG) through floodwater spreading (FWS) which is a potential measure for reversing this emerging trend is investigated in this research. The overall objective of this dissertation is to evaluate a floodwater spreading system that was installed in 1981 at the Gareh Bygone Plain, southern Iran for recharging the groundwater table. The main research objectives are i) to assess the recharge of the groundwater by the floodwater spreading system using a combination of two types of saturated zone methods, water table fluctuation (WTF) and water budget, and ii) to assess the recharge by the same system using a vadose modelling approach based on soil water content measured over the vadose zone using probes that were particularly calibrated for the stony layers of interest.

In a first 'saturated zone' approach, The recharge was calculated at 7.94 Mm3, which was a consequence of both artificial recharge and natural replenishment. The artificial recharge data in the same period during the flooding events from 28 January to 2 February 2011 show a total volume of 6.92 Mm3 of retained flood water in the FWS systems. Artificial recharge from these events, which ponded an average depth of 0.34 m on the system surface, was calculated as 0.24 cm. The artificial recharge was calculated by the two methods (flow data and water budget, respectively) as 4.84 and 4.46 therefore, 56 to 61% of the recharge could be assigned to the impact of the FWS systems for this hydrological year.

In a second 'unsaturated zone' approach, recharge of the groundwater table was evaluated by measuring and modelling water content within the vadose zone inside the FWS systems. Calculations using the soil water balance and Hydrus1D methods, indicated that out the 51.8 cm of rainfall and ponded floodwater added to the site during the 16 January to 23 August 2011 period, 29.6 cm of cumulative flux (recharge) occurred, showing an efficiency of 57%. To recapitulate briefly, it might be concluded that, notwithstanding the decline in groundwater table observed in recent decades in the Gareh Bygone Plain, the FWS systems that was installed there in 1981 seems to be effective in recharging the groundwater table. Two independent approaches suggest that 57 to 61% of rainfall effectively flows to the groundwater table.

Keywords:

Soil water balance, Hydrus1D, Floodwater Spreading, Recharge Assessment.

Introduction

ACCORDING to Wada et al. (2010), the estimated extent of GW depletion in sub-humid to dry regions has grown from 50 to 115 ($km^3 ha^{-1}$) between 1960 and 2000, whereas the withdrawal of water from the GW has increased unequally from 125 to 295 km^3 ha^{-1} in the same period. This means an increase at factor 2.25 and 2.38 for depletion and withdrawal, respectively. It reveals that a part of withdrawn GW is being compensated by recharge (natural and artificial), but there is no guarantee that the proportion of recharge/withdrawal will remain stable to keep the current trend of depletion (Hashemi, 2015). This fact declares the importance of quantification the recharge and its proportion to depletion especially in the regions with significant reliance of food production to the GW. Floodwater harvesting systems have been mainly assessed in terms of supporting rainfed farming rather than their contribution to ARG. As new applications of FWH techniques aim at GW recharge, GW studies seem to be a new area of research for FWH evaluation and assessment (Sanford, 2002). However, adequate estimation of recharged water is often difficult due to complex geophysical features and the large temporal and spatial variability of rainfall and runoff (Rushton and Ward, 1979; Sophocleous, 1991; Flint et al., 2002). Floodwater spreading (FWS) systems is one of the important measures of water management in dry regions. Few works is found on assessment of the FWS systems impact on groundwater augmentation. Despite the long and successful history of these systems, little is still known about their function and effect on hydrological processes in dry areas (Ouessar et al., 2009; Hashemi et al., 2015; Pakparvar et al., 2018). Nevertheless, the rate of aquifer recharge is one of the most difficult elements to measure in the evaluation of GW resources (Sophocleous, 1991; IGRAC, 2017). The overall objective of this integrated study was to evaluate a floodwater spreading system that was installed in 1981 at the Gareh Bygone Plain, southern Iran for recharging the groundwater table. The main research objectives are i) to assess the recharge of the groundwater by the floodwater spreading system using a combination of two types of saturated zone methods, water table fluctuation (WTF) and water budget, and ii) to assess the recharge in the same system using a vadose modelling approach based on soil water content measured over the vadose zone using probes that were particularly calibrated for the stony layers of interest.

Materials & methods

A. Site description

The Gareh Bygone Plain has an area of 18000 ha. The FWS project area comprises 2033 ha (area under water spreading). Very little freshwater resources were available before the artificial recharge of the GW through the FWS activities, which started there in 1983.

It is located south of Zagros Mountains, Southern Iran, between 28º 35' to 28º 41'N and 53º 53' to 53º 57'E. The altitude of the plain ranges between 1120 and 1160 m a.s.l. (Fig. 1). A dry region, with mean annual precipitation of 211 mm, having high inter-annual variability. Rainfall mainly occurs from December to March, with few exceptional events in summer (June-August). The absolute maximum temperature (40-46ºC) occurs in July-August and the corresponding minimum (-1 to -6ºC) in January–February.

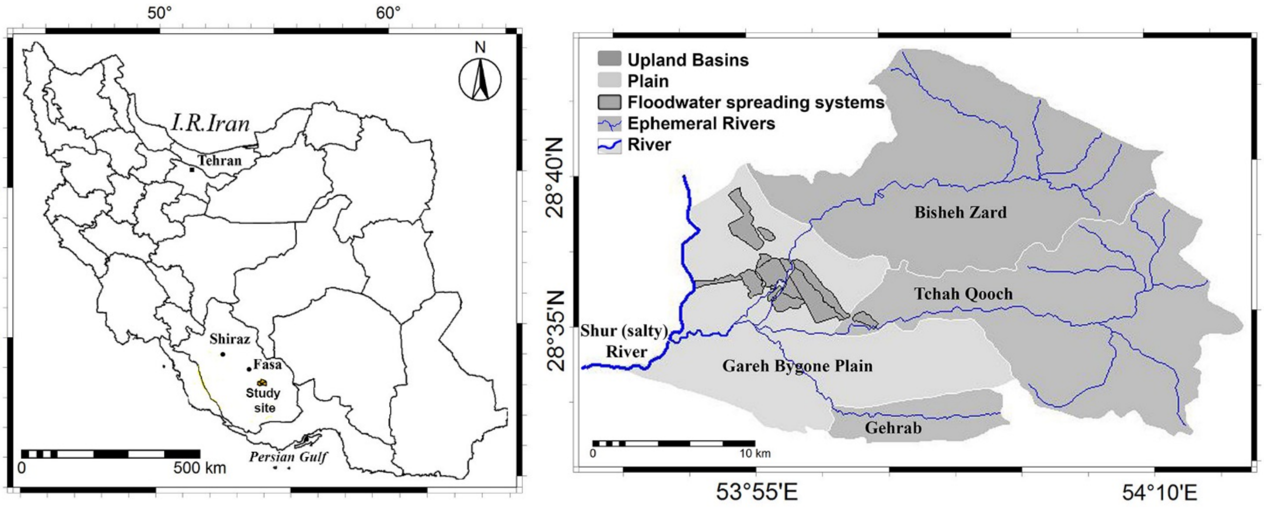

Fig. 1. Location of the study site in Iran (top) and a map of floodwater spreading (FWS) systems on the Gareh Bygone Plain (GBP) and its upland Basins (bottom).

B. How floodwater spreading system works

The Kowsar Station was established in 1983 with the aim of desertification control through FWS (Kowsar, 1991). The FWS systems were planned following the methods pioneered by Philip (Philip, 1957), improved by Newman (1963) and Quilty (1972), and modified by Kowsar (1991). Eight FWS systems with an extent of 1236 ha were constructed during the 1983-1985 period. Expansion of the FWS systems to 2033 ha was performed from 1996 to 2003. The names and locations of the FWS systems on the Gareh Bygone Plain are presented in Fig. 1. However, the entire FWS systems are not covered by floodwater in all of the events, at least one event occurs in non-drought periods which results in full coverage of the systems. Our experience shows that the flooding events of flow rate higher than 100 m3 s-1 in Bisheh Zard River cause a complete coverage of the systems.

A diagram is presented in Fig. 2 to illustrate a typical FWS system and its essential components. A FWS system starts with a diversion dam which is constructed on the river bed widthwise with a spillway to deliver a pre-defined discharge of the flow to the diversion gap. Flow in turn, reaches the beginning of the FWS system via a conveyor canal. As this canal acts simultaneously as a sedimentation basin, does not include the upslope bank and the flow inundates the upstream of the bank which causes a decrease in flow velocity, it is called as inundation canal. The flow then enters to the most important element of the system that is a dual purpose conveyor-spreader channel which transfers water to the head of the spreading area and, ideally, distributes it evenly onto the land.

This channel is actually a long, shallow stilling basin which converts some of the kinetic energy of the flowing water into potential energy, thus elevating the level of the water surface a few cm above that of the lower sill of the channel, with the resultant flow of a shallow sheet of water on a very long front. The excavated soil forms a bank on the upslope side of the channel. Openings or weirs are provided in the bank to facilitate entrance of water into the channel during major floods when flows, larger than the capacity of the conveyor-spreader channel, bypass the junction of the diversion canal and the channel and flow along the topside of the bank. Water is supplied to the conveyor-spreader channel by a diversion, or an inundation canal. It is imperative to realize that the conveyor-spreader channel is the only structure in the system which is connected to the river.

The spillage from the conveyor-spreader channel flows over the land in a sheet whose depth and velocity depend on the flow rate, slope, infiltration capacity, sediment concentration, soil and water temperature, ground cover, etc.

The depth of water on the sill of the conveyor-spreader channel, which also depends on the foregoing factors, is usually 3-5 cm, rarely exceeding 10 cm. The terminal velocity of a 10 cm sheet of water on a 2% slope on denuded land seldom exceeds 60 cm s-1. At this depth and velocity the flow is non-erosive for all practical purposes. The flow of water on the land is regulated by the level-silled channels which are closed at both ends. These channels, which are located at 140-250 m spacing downstream of the conveyor-spreader channel, function as described for the conveyor-spreader channel with two exceptions. First, they receive water only through the gaps provided in their banks at 100-400m intervals; thus in low flows or short duration floods they may receive no water to spread.

Second, they are level along their entire lengths so they spread the water more evenly. When floodwater reaches the end of a floodwater spreading system it has lost most of its sediment load and is suitable for artificial recharge, or filling up surface reservoirs (Pakparvar, 2015).

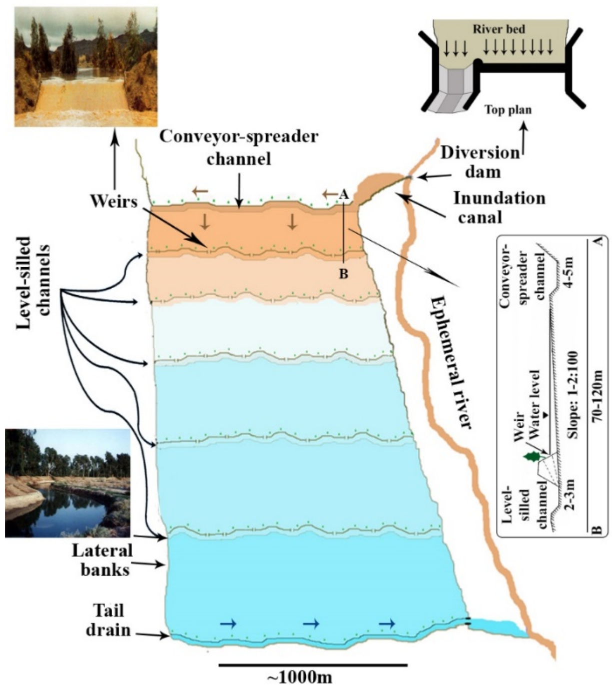

Fig. 2. Generalized diagram of a typical floodwater spreading system. The scales are approximate.

C. Data collection setup

Water table level and weather data

Installation of observation wells (OW) in the study area started in 1992 (Fig. 3). Well Nos. 1 and 4 (OW1 and OW4) are located outside of the FWS systems. OW2, OW5, and OW6 are situated inside, and OW3 immediately downstream of the FWS systems. OW5 and OW6 were installed in 2005. None of the OWs are located within 200 m distance of operational wells so, there was no effect of lateral in and out flow to the OW as influenced by active pumping zones of adjacent wells. The criteria of 200 m distance is defined by the responsible authority (Water Resources Research Organization) in Iran as a guideline for observation wells installation. Observation wells data include the height of the measuring point (MP) from the mean sea level, and depth of the WT relative to the MP during 1993-2012. The depth to WT was measured on a monthly basis from 1993 to 2012 by the Fars Regional Water Organization (FRWO) using an ordinary water level meter with light indicator and a resolution of 0.01 m. Weather data were available at the Gareh Bygone Weather Station from 1996 to 2017. Rainfall data for the 1992-1996 period were collected from the nearest climatologic station (Baba Arab), 15.75 km from the Kowsar Station.

Runon and runoff data

The volume of floodwater diverted to the FWS systems from January 1983 to November 2002 has been estimated and reported by the responsible authority of the Kowsar Station (internal technical reports). Due to a complete lack of data and instrumentation before 2002, the peak flow rates have been calculated by using empirical slope-area method as discussed in the following section.

From November 2002, there have been two types of flow measurements in the FWS systems in the study area. First, peak flow was recorded at the hydrometric station and second, diverted flow inside the FWS systems was measured by broad-crested weirs.

Experimental wells

Three experimental wells (EW) were hand dug in locations with different land covers, i.e., tree plantations (TP), pastures inside FWS system (PI) and bare soils (BS) (Fig. 3). The objectives of installing the three wells were: a) to identify profile layers of the basin, b) to determine hydraulic properties of the layers, c) to equip one of the wells with TDR probes. The wells were dug until the water table level (28.8 to 31.6 m) and had a diameter of 120 cm for easy access into the wells. The difference in depth of the wells is attributed to the difference in the months of excavation (from May to August) as the GW level falls during this period.

The FWS systems used as the research site was constructed in 1983. A top layer of silt loam, 10 to 20 cm thick, had been formed over the original soil surface due to the deposition of the suspended load during 30 years of being used as sedimentation basin in which the recharge also takes place simultaneously. The observation well through which the collected data analyzed in this study is located at 50 m distance from the upstream level-silled channel and 60m from the downstream one.

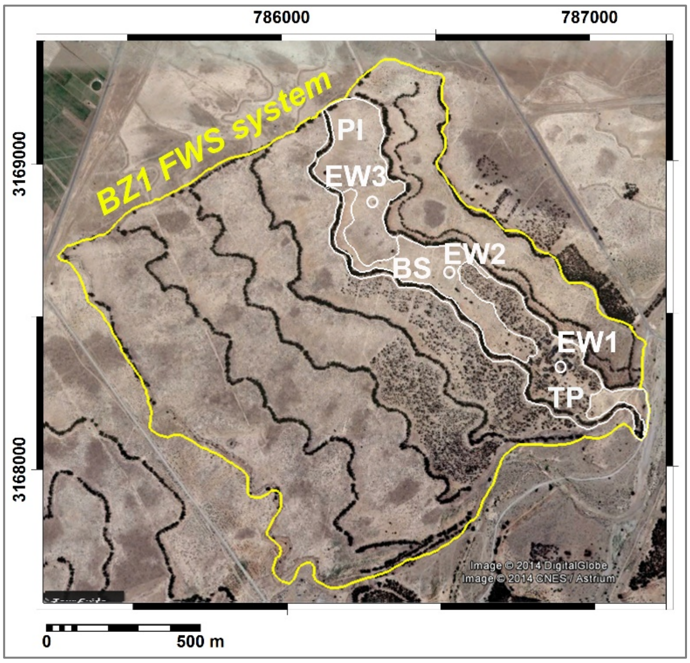

Fig. 3. Location of BZ1 FWS system and land cover of the 2nd basin; TP is tree plantations, PI is pastures inside the floodwater spreading system and BS is bare soils. EW1 to EW3 are experimental wells (1-3).

Soils

Soils of the study basin, which is formed on a debris cone and the alluvial fan developed by the BZ Ephemeral River, is covered with a layer of drifting fine sand ranging in thickness from a few mm to several cm. A structureless, coarse sandy loam with average sand, silt and clay contents of 73.2, 14.5 and 12.2%, respectively forms the A horizon, 10-20 cm thick. The stony C horizon lies directly under the A horizon. It has been classified as coarse-loamy skeletal, carbonatic (hyper) thermic, Typic Haplocalcids (Kowsar, 1991; Soil-Survey-Staff, 2010).

Water ponding measurement

The time at which the area surrounding the experimental wells was pounded by floodwater and the height of ponding water were recorded. The height was measured by an in-built ruler in each one hour interval.

Field saturated hydraulic conductivity

The field saturated hydraulic conductivity K_{fs} was measured by the double ring method (Reynolds et al., 2002) using two rings with inside diameter of 0.30 and 0.59 m, respectively in well number 1 during its construction.

The K_{fs} was measured for each 30 cm increment from the soil surface down to 3 m, and for each 100 cm increment from 3 m down to 30 m. The rings, 0.40 and 0.25 m high, were driven into the soil to a depth of 0.03-0.05 m, respectively. The soil surface in the inner ring was covered with a plastic sheet to prevent soil disturbance. Water was added cautiously to both the inner and outer ring until a 20 cm water depth was reached; the plastic sheet was then removed from under the inner ring. The falling water depth in the inner ring was recorded using a ruler after 1, 3, 5, 10, 15, 25, 35, 55 and 75 minutes, i.e., for at least 75 minutes or until the infiltration rates in the successive time intervals remained practically constant.

Bulk density

Upon completion of each infiltration measurement in well number 1, bulk density was measured inside the inner ring. Because of stoniness of many layers, the core method was not applicable and the excavation method modified based on Grossman and Reinsch (2002) was applied for all of the layers. At each depth, a cavity with a rough volume of 2500 cm3 was dug and insulated with a plastic liner. The excavated material was collected, oven dried and weighed before and after drying. The exact volume of the cavity was measured by adding a measured volume of water into it. Bulk density was then calculated by dividing the dry weight of the bulk materials (soil and stone) by the cavity volume.

Particle size analysis

Bulk material of every depth was collected and texture of the material <2 mm was determined in the laboratory using the sieving and hydrometer method in order to better distinguish the layers. Two kg of each sample was used to particle size analysis. This was carried out using the hydrometer method combined with sieve analysis to characterize the range of particle diameter from 0.002 up to 2 mm (Gee and Or, 2002). Stone fraction (>2mm) was determined by the sieving method.

Identifying and correlating the wells' profile layers

The data set of the hydraulic properties, soil texture and stoniness, of the different depths was used as the basis for differentiation between the layers of the profile of the experimental well number 1. The whole dataset is presented in Appendix 5. Then, a visual description of the profile layers in the three wells was made by descending inside the wells. Alphabetic codes (A to G) were assigned to seven representative layer (RL). Then the distribution (thickness and location) of every code over the wells' profile was determined to prepare the log of each well. The logs of the three wells were then correlated to match the congruent layers and to find the horizontal distribution of the aquifer layers in the study area.

The specified layers in the three wells were analyzed in order to recognize the correspondence between the RLs and their distribution over the wells' profile. Hence, a correlation between the horizontal layers was made to produce a 3D imagine (2D vertical distribution of the layers in different wells).

Installing the TDR probes

The Trase System 6050X1 (Soilmoisture Equipment Corp., USA) was used for soil water content measurement. It is a TDR-based system which was first calibrated for the main soil types of the study area. The main steps in installing the system were as described below.

To install the three-rod TDR probes, which were manufactured and tested in this study, small openings were made in the concrete tiles to have access to the vadose zone behind. In order to prevent probe damage, and also to ensure good soil contact, a mold of TDR probe was fabricated, which was first inserted into the soil. This facilitated easy and tight insertion of the TDR probes. Probes were installed approximately at the same depths at which infiltration measurements were made. From top to well bottom, probes were installed at 0.1, 0.4, 0.6, 0.8, 1.1, 1.4, 1.7, 2, 2.3, 2.6, 2.9, 4, 5, 6, 7, 8, 9, 10, 12, 14, 16, 18, 20, 24, 26, 28 m depths. They were connected to the desired extension cables (if needed) and each cable was driven to the top of the well by its unique guidance polyethylene pipe. The pipes were organized and numbered in order to have easy access to each probe's depth.

Soil water content measurement

The data collection spanned from 21 August 2010 to 1 December 2015. Measurements were taken manually by connecting each probe to the main device and reading the data. Both the measured dielectric permittivity (K_a) and the estimated volumetric SWC ($m^3\ m^{-3}$) were recorded and stored in the TRASE device. Measurements were performed at 6-8 day intervals before rainfall and/or flood occurrence, twice daily for 30 days during and after such events, and daily thereafter until returning to the prior SWCs of previous events. There were some missing data at some pre-planned time intervals owing to the logistical shortcomings.

ET data

The actual daily ET (ETa) was generated by a combination of the FAO Penman-Monteith (FAO P-M) and remote sensing based on the SEBS model. The details are presented in chapter 3 of this thesis. The starting date on which the ETa was measured by the SEBS model was 21 December 2010 (Pakparvar et al., 2014).

D. Assessment of recharge

Hydrologic balance

The method used by Hoque et al. (2007) was applied for estimating recharge in a particular duration of time (Eq. 1). This analysis was performed for the hydrological year 2010-2011 as the complete data necessary for the analysis was only available for that hydrological year. Eq. (3-2) was solved to find the recharge (*R*) as a remainder when the other components such as extraction from the aquifer (*E*), change in GW storage (ΔS) and return flow (*RF*) are known.

$$R = E + \Delta S - RF + ET^{gw} \qquad (1)$$

ET from the GW (ET^{gw}) was considered as the water consumption by the tree plantations which have access to GW by their deep roots.

Application of flow data

The part of water in a recharge pound consumed by total losses (open water evaporation plus *ET*), when subtracted from the amount of pounded water, is net total infiltration (Hendrickx et al., 1991).

it should be noted that the horizontal hydraulic conductivity of aquifers similar to the aquifer in our study (medium to coarse gravelly material) is reported as 0.02 to 1.02 cm day^{-1} (Domenico and Schwartz, 1990) whereas the vertical hydraulic conductivity measured in this study varied between 17 to 2840 cm day^{-1} which is by far higher than the expected horizontal hydraulic conductivity. Therefore, the assumption of neglecting lateral movement at least when vertical infiltration due to a flooding event is in progress is reasonable.

The evaporation losses during a given period depend on the duration of infiltration and, therefore, on the infiltration rate. To evaluate the recharge, the equation derived by Hendrickx et al. (1991) was used:

$$AR = D - eD/(i + e) - \sum ET \qquad (2)$$

where, i is the infiltration rate (mm day^{-1}), e is the open water evaporation during the period of infiltration (mm day^{-1}), $\sum ET$ is the cumulative *ET* after all water has infiltrated (mm), A*R* is the net artificial recharge (mm), and *D* is the depth of water applied for recharge (mm).

Soil-water budget approach

The soil-water budget equation can be written as (Evett et al., 2012):

$$R = P + I + F - \Delta S - ET_a + \varepsilon_R \qquad (3)$$

where *R* is deep recharge, *P* is precipitation, *I* is irrigation, *F* is flooding which means runoff minus runon, ΔS is the change in soil-water storage over the considered time period, ET_a is actual *ET* and ε_R is a function of the errors in determination of ΔS, *I*, *P*, *R*, and *F*.

SWC measured per depth (θ_v × thickness of each layer) was summed up for all of the layers as total storage (*S*) in each day and the change in SWC (ΔS) was calculated by subtracting the *S* of the successive days. The ΔS of the layers were then used to calculate the soil-water storage within the vadose zone. Records of the pounded floodwater on the soil surface close to the well during the flooding events were considered as remainder of runoff and run on in the system. Then Eq.

(3) was solved for recharge *R* on a daily basis. The period between the time at which the SWC of any layer started to increase due to the flooding event and the time of returning back to its previous normal level (SWC of all layers before the event) was set as the calculation period. Summation of the daily recharge data during the calculation period was considered as the net recharge due to that particular event.

Results & discussion

Piezometric level and flow directions

The GW level of the Bisheh Zard aquifer and the GW flow direction is presented in Fig. 4a. The water level data of the six OWs together with the collected water level of the operational wells in the year 2012 corresponding to the Bisheh Zard aquifer were used to prepare the maps.

The piezometric contour lines start at its highest value of 1165 m.a.s.l at the Northeast, decline gradually to 1115 m.a.s.l under the zone of FWS systems activity and show a concave shape in this area which is a sign of influence of artificial recharge. The contours continue to descend to 1105 to 1100 m.a.s.l at the South to Southwest part in the vicinity of Shur River. The rate of decline is proportional to the surface topography (Fig. 4b) which means that the GW topography follows the soil surface topography. The GW flow in the aquifer (Fig. 4a) shows a direction from upland to lowland and eventually to the Southwest and West where the Shur River drains the aquifer. A different minor local directions is also seen in Southern part from the Tchah Qooch River to the North direction which corresponds to the recharge from the mentioned River.

Recharge estimation

Results of extraction are presented in Table 1. Applied agricultural water and withdrawal estimation were 13.82 and 15.27 Mm^3, respectively. These two methods of extraction estimation resulted in different but close values as some of the extracted water is not used as irrigation application and is lost during transport within the earth canals between the farm fields. The amount of loss is 1.45 Mm^3 or 9.5% of the withdrawn water. Therefore extraction volume based on the withdrawal water (15.27 Mm^3) was chosen as the basis for further calculations (Table 2).

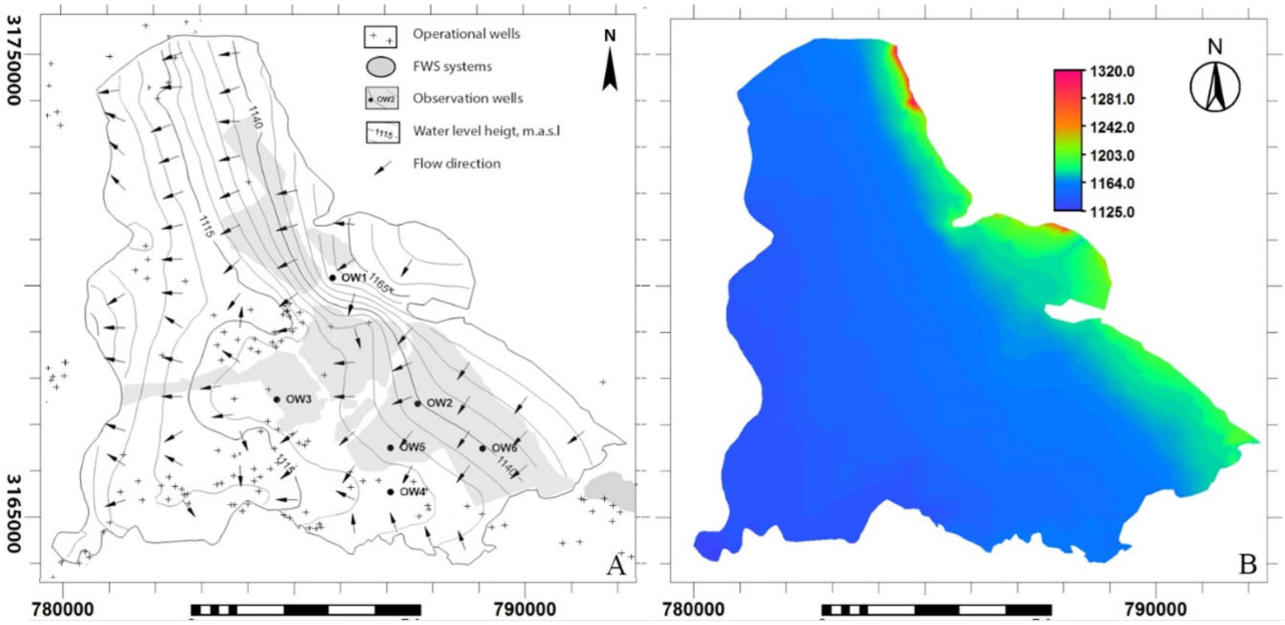

Fig. 4. Piezometric map (A) and the digital elevation model (DEM) map (B) of the Bisheh Zard aquifer.

Table 1.
Calculations of water extraction in the hydrological year October 2010 to September 2011.

Consumers	**Area, ha**	**Ave. applied, $m^3 ha^{-1}$**	**Consumption, Mm^3**
Based on measured applied water			
Winter crops	1184	4800	5.68
Summer crops	725	9800	7.11
Tree plantations	132	7450	0.98
Domestic use			0.05
Sum			13.82

Based on water withdrawal

Sources	**No. wells** Total	Active	**Mean discharge,** $L s^{-1}$	**Mean working times,** $Hr yr^{-1}$	**Abstraction,** Mm^3
Wells	148	88	7.95	5655	14.24
Tree plantations					0.98
Domestic use					0.05
Sum					15.27
Transport losses%					10.3

[1]Applied water for tree plantations is calculated by the ET_a mapping. The water consumption of tree plantations is considered as a source of GW extraction due to their roots access to the GW table (observed in this study at the depth of 28 m. Mm^3 is million m^3. The total extraction by water withdrawal was calculated for every well's discharge and working hours and summed up for the all wells. The means are shown here to be indicative of the wells' discharge and working times. Transport losses is calculated as the ratio irrigation applied/withdrawn water (5.68+7.11)/14.24.

Table 2.
Water budget of the total recharge in the hydrological year 2010-2011.

Inputs, Mm^3		**Outputs, Mm^3**	
ΔS	4.13	E	15.27
RF	3.20		
R	7.94		
Total	15.27		15.27

ΔS is change in GW storage, R is recharge, RF is return flow, E is total extraction from the GW, Mm^3 is million m^3. R is calculated as the remainder of the water budget Eq. (3-7).

Artificial recharge estimation

i) Based on the flow data

The artificial recharge data in 2010-2011 are presented in Table 3. During the flooding events from 28 January to 2 February 2011, a total volume of 6.92 Mm^3 of flood water was retained in the BZ FWS systems. These events ponded the entire FWS systems of 2033 ha (22.33 Mm^2) and resulted in an average depth of 0.34 m on the FWS surface. The duration of the infiltration was counted as 6 days, evaporation rate (e) as 0.024 m day^{-1}, the sum of ET ($\sum ET$) after the event for the 30 days was calculated as 0.075 m, weighted average of infiltration rate (i) was calculated as 0.28 m day-1 and therefore, the recharged water was estimated as 0.24 m (Table 3).

As a results, the volume of artificial recharge due the FWS on the 20.33 Mm^2 of the FWS systems was estimated as 4.84 Mm^3. The ratio of artificial recharge to the depth of ponded water (0.24 and 0.34, respectively) was 0.7. Hendrickx et al. (1991) reported similar values (0.6 to 0.8) for an alluvial stony fan resembling our study site.

Table 3.
Flow rates of floods diverted into the FWS systems in 2011.

Flooding date	Mean Discharge, $m^3 s^{-1}$	Duration, hr	In-flow (Mm³)	Out-flow (Mm³)	Retained flow (Mm³)
28-Jan-11	115	3	1.24	0.25	0.99
1-Feb-11	159	13	7.44	4.62	2.82
2-Feb-11	203	8.5	6.21	3.10	3.11
sum			14.90	7.97	6.92

In-flow and out-flow are the volume of incoming and outgoing flood flow to the floodwater spreading system. Retained flow is the volume of flood flow retained by the system.

TABLE 4.
COMPONENTS OF THE RECHARGE CALCULATION BASED ON THE FLOW DATA.

Retained flow, Mm³	Area, ha	*D*, m	*e*, m day-1	*i*, m day-1	*∑ET*, m	*AR*, m	*AR*, Mm³
6.92	2033	0.34	0.024	0.28	0.075	0.24	4.84

D is depth of ponded water, *e* is evaporation rate, *i* is infiltration rate, *∑ET* is the sum of *ET* in the 30 days after flooding event, *AR* is artificial recharge.

ii) Based on the water budget

The surrounding area has a size of 3232 ha and volume of GW rise was calculated at the 9.03 Mm³. According to the determined S_y as 0.18, the volume of change in GW storage due to the artificial recharge (ΔS) was obtained as 1.625 or ~1.63 Mm³. During the three months after the event (the period which was considered for GW rise), some part of recharged water was used as irrigation water and consumed by tree plantations The size of cultivated area of the farmlands located inside the FWS systems influencing boundary was measured as 705 ha, the rate of applied irrigation was considered as 4800 m^3 ha^{-1} hence, the extracted volume of irrigation water was obtained as 3.38 Mm³. The amount of extracted water by tree plantations was calculated based on summed up ET_a in the same period as 2300 m^3 ha^{-1}.as the 0.30 Mm³. As the amount of *RF* was obtained as 22.5%, the volume of *RF* was calculated as 0.73 Mm³ (22.5% of the 2.95 Mm³ crops irrigation + 0.31 Mm³ transport losses) and therefore, the artificial recharge is estimated as 4.46 Mm³ (Table 5).

Table 5.
Water budget of the January to April 2011 for the area under the immediate influence of FWS systems.

Inputs, Mm³		Outputs, Mm³	
AR	4.46	*E*	3.56
RF	0.73	Δ*S*	1.63
Total	5.19		5.19

Δ*S* is change in GW storage, *AR* is artificial recharge, *RF* is return flow, *E* is total extraction from the aquifer, Mm³ is million m³. AR is calculated as the remainder of the water budget Eq (1).

The contribution of the artificial recharge is calculated as 4.84 and 4.46 Mm³ by the flow data and the water budget, respectively. The lower value obtained by the water budget method is expected as it is essentially based on the change (rise) in GW storage as influenced by the net recharge of the groundwater and the one obtained by the flow data is based on the total infiltrated water to the deep layers. Consequently, the difference between the two values appear to be the portion of the net infiltration (7% of 4.84 Mm³) which had not contributed to recharge and is moved horizontally. Conditional to selecting one of the resulted values to the artificial recharge, 56 to 61% of the total recharge could be attributed to the impact of the FWS systems for that hydrological year.

iii) Based on SWB method

As inferred from Table 6, the rainfall and flooding event that started on 28 January 2011, caused an increase in soil-water storage *S* of the top 400 cm layers from 10.80 to 19.33 cm. Flooding continued until 1 Feb 2011, and the increase in *S* of the top 400 cm reached 35.18 cm on that day. The profile's *S* decreased gradually afterwards until 23 July, when total *S* had decreased to 11.54 cm, close to its amount before the flooding event. Summation of the difference in soil-water storage between two measurements ΔS for the entire period should approach zero. ET_a values are daily based for the successive days of the SWC measurements and the cumulative for the intervals of non-successive days (Table 6).

As shown in Table 6, the remainder of ΔS for the entire period was 2.0 cm, which means that the total water infiltrated into the profile in terms of rainfall and floodwater (51.8 cm) had left the profile as either *ET* or recharge. As ET_a was calculated as 20.2 cm, the net recharge depth to the aquifer was estimated at 29.6 cm for that particular event.

Table 6.
Soil-water budget data from the 400 cm top layers, the flooding period 16 January to 23 July 2011.

Dates	*S*	*ΔS*	*P*	*F*	*ET*
	----------	----------	cm	----------	----------
1/16/11	30.0	0.0	1.2	0.0	0.0
1/23/11	35.4	5.4	2.9	0.0	0.9
1/28/11	40.1	4.7	2.9	0.0	1.0
2/17/11	58.7	-1.1	0.0	0.0	0.2
2/18/11	59.0	0.3	0.4	0.0	0.0
..	..	..	..	..	..
6/28/11	32.9	-0.3	0.0	0.0	0.2
7/12/11	33.0	0.0	0.0	0.0	0.0
7/23/11	32.5	-0.5	0.0	0.0	0.3
7/30/11	32.0	-0.5	0.0	0.0	0.3
1/16/11 to		**2.0**	**16.8**	**35.0**	**20.2**
Recharge (cm) in entire period: R=P+F-ΔS-ET					**29.6**

The data is continued from the 2/18/11 until 6/28/11 but is not shown to abstract the table.
S is soil-water storage summed up for 400 cm top layers, *ΔS*, is change in soil storage as subtraction of measured *S* for each day from the last previous measured *S, P* is precipitation, *F* is flooding and ET_a is actual *ET* which is cumulative for the non-consecutive days.

It can be inferred from the θ_v data set that the decrease in hydraulic conductivity due to clogging by siltation in the studied artificial recharge system did not affect its efficiency, at least at the experimental site. The fact that the wetting front arrived at a depth of 400 cm after 48 hours from the start of the flooding event clearly challenges the assumption of negative impact of surface clogging on infiltration. As the wall of the well was primarily insulated by concrete tiles, there was no possible lateral movement of water to the well; hence, the change in the SWC can only be attributed to the vertical movement of water as influenced by the vertical infiltration of rainfall and/or ponded water.

The SWC time series, the concurrent collected ponding water, rainfall and the remotely sensed ET_a data were used to solve the soil-water budget approach for a period of 188 days. In this period the initial SWC of the soil layers increased in response to the rainfall and/or flooding events from the top to the underlying layers successively and thereafter started to decrease due to *ET* and recharge until reverting to its initial value.

Consequently we can consider the amount of 29.6 cm resulted by soil-water budget method as the reliable outcome of recharge calculation of this study. Hence, from the 51.8 cm of input water (16.7 and 35.0 cm rainfall and floodwater, respectively), 29.6 cm (57%) moved below 400 cm depth to follow its downward movement to the aquifer. The amount of artificial recharge which was calculated in this chapter is comparable to that was evaluated in the chapter 3. In the both methods the amount of pounded floodwater plus rainfall was considered as the input water and the part of infiltrated water to the deep layers were evaluated. In the chapter 3, conditional to the method used, 56 to 61% of the input water was estimated as artificial recharge. Similarly, in a silty clay loam with a fragmented layer below 60 cm, (Soldevilla-Martinez et al., 2013) calculated the drainage from the profile bottom at 170 cm depth as 70% of precipitation and ponding water using the soil-water budget method. On the contrary, some reports show lower recharge percentage; for instance, Touhami et al. (2013), calculated recharge to be 4 to 28% of precipitation in a fine-textured soil with different land cover types using three soil-water budget models. Bellot and Chirino (2013) calculated recharge due to net precipitation (precipitation minus interception) as 30 to 51% in wet years, and 8 to 30% in dry years in a forest with fine textured (clay loam) soil. Webb et al. (2008) calculated recharge by the LEACHM model as 9 to 13% of the annual precipitation (1200 mm). The main difference between our study and those presenting low recharge percentages can be ascribed to the type of input water. In our study, the summation of rainfall and the ponded floodwater were the sources of input, which play a major role in the recharge efficiency. In addition, the hydraulic properties of the soils under study in our site are characterized by coarse and gravelly texture, and therefore, show higher hydraulic conductivity and lower water retention in comparison with the above mentioned reports.

Conclusion

Saturated zone approach

In the saturated approach, we firstly examined the immediate impact of FWS on the water table level. The observation wells (OW) inside the FWS system showed a twice as high response to the flooding event in comparison with the OW outside the system. Tolerance against groundwater (GW) extraction lasted for OWs inside the FWS much longer than those outside the FWS system. We further employed a combination of water budget and water table fluctuation (WTF) methods to solve for recharge by quantifying all of the involving components. Considering that the calculated 4.13 Mm3 was depleted from the aquifer storage during the hydrological year 2010-2011, and the return flow as 3.20 Mm3, the recharge was calculated at 7.94 Mm3 in that year, which was a consequence of both artificial recharge and natural replenishment.

Artificial recharge data in the same year during the flooding events from 28 January to 2 February 2011, showed a total volume of 6.92 Mm3 of flood water that was retained in the FWS systems. The calculated artificial recharge was calculated at 4.48 and 4.46 Mm3 by the methods of using flow data and the water budget, respectively, from these events. Therefore, the contribution of the FWS systems to recharge was calculated as 56 to 61% for this hydrological year. This ratio is similar to those reported by (Hendrickx et al., 1991) who found values of 60% to 80% for an alluvial stony fan resembling our study site. Moreover, in a parallel study in our study area (Gareh Bygone Plain), (Hashemi et al., 2013) showed, using a numerical hydrologic modelling, that the contribution of the FWS systems to the recharge is 80% in normal events and 41% in extreme events.

Unsaturated zone approach

In unsaturated approach, after calibrating the TDR method for the stony soils of the studied aquifer layers, a soil-water budget (SWB) method was employed to simulate the recharge in a period between 16 January 2010 to 30 July 2011.

In this period the SWB method showed that the total water infiltrated into the profile in terms of rainfall and floodwater (51.8 cm) had left the profile as either ET or recharge and a soil-water storage of 2.0 cm was retained in the profile layers. The cumulative ETa was calculated as 20.2 cm and therefore, the net recharge was estimated at 29.6 cm for this period. Therefore, from the 51.8 cm of input water, 29.6 cm was net recharge, which shows an efficiency of 57% for the system. This value is valid for the experimental site, which is considered as being representative for the BZ1 FWS system under study.

Integration of the results

In spite of the persistent lowering of the GW level in recent decades, the efficiency of the system was quantitatively evaluated as 58-63% and 57% by the saturated and unsaturated zone approaches, respectively. This is supported by a parallel study by Hashemi (2014), who introduced different water management scenarios to assess the impact of management parameters such as size of FWS system, GW extraction and climate change on the GW level in the coming years. The scenarios revealed that abstraction most substantially affects the GW level and the continuation of abstraction at the current pumping rate would lead to a GW decline by 18 m up to 2050. Their results show that the recharge volume can be increased by expanding the artificial recharge system, even for small flood events, while recharge through the river channel is only substantial for major flood events.

Therefore, extension and development of FWS systems in the studied area would be a main and permanent solution to increase the floodwater recharge in case of any extreme or small flash flood event.

References

- Bellot, J., Chirino, E., 2013. Hydrobal: An eco-hydrological modelling approach for assessing water balances in different vegetation types in semi-arid areas. Ecological Modelling, 266(0): 30-41. DOI:http://dx.doi.org/10.1016/j.ecolmodel.2013.07.002
- Domenico, P.A., Schwartz, F.W., 1990. Physical and chemical hydrogeology. John Wiley & Sons, New York.
- Evett, S.R., Schwartz, R.C., Casanova, J.J., Heng, L.K., 2012. Soil water sensing for water balance, ET and WUE. Agricultural Water Management, 104(0): 1-9. DOI:http://dx.doi.org/10.1016/j.agwat.2011.12.002
- Flint, A., Flint, L., Kwicklis, E., Fabryka-Martin, J., Bodvarsson, G., 2002. Estimating recharge at Yucca Mountain, Nevada, USA: comparison of methods. Hydrogeology Journal, 10: 180-204.
- Gee, G.W., Or, D., 2002. Particle-size analysis. In: Dane, J.H., Topp, G.C. (Eds.), Soil Science Society of America Book Series: vol. 5, Methods of Soil Analysis. Part 4: Physical Methods. American Society of Agronomy, Madison, WI, pp. 255-293.
- Grossman, R.B., Reinsch, T.G., 2002. Bulk density and linear extensibility. In: Dane, J.H., Topp, G.C. (Eds.), Methods of soil analysis, part4: Physical methods. SSSA Book Ser. 5. SSSA, Madison WI, pp. 201-228.
- Hashemi, H., 2015. Climate change and the future of water management in Iran. Middle East Critique: 1046706. DOI:http://dx.doi.org/10.1080/19436149.2015.1046706
- Hashemi, H., Berndtsson, R., Kompani-Zare, M., Persson, M., 2013. Natural vs. artificial groundwater recharge, quantification through inverse modeling. Hydrol. Earth Syst. Sci., 17(2): 637-650.

DOI:http://dx.doi.org/10.5194/hess-17-637-2013
– Hashemi, H., Berndtsson, R., Persson, M., 2015. Artificial recharge by floodwater spreading estimated by water balances and groundwater modelling in arid Iran. Hydrological Sciences Journal, 60(2): 336-350.
– Hendrickx, J.M.H., Khan, A.S., Bannink, M.H., Birch, D., Kidd, C., 1991. Numerical analysis of groundwater recharge through stony soils using limited data. Journal of Hydrology, 127(1–4): 173-192. DOI:http://dx.doi.org/10.-۹۰۱۱۴(۹۱)۱۶۹۴-۰۰۲۲/۱۰۱۶W
– Hoque, M.A., Hoque, M.M., Ahmed, K.M., 2007. Declining groundwater level and aquifer dewatering in Dhaka metropolitan area, Bangladesh: causes and quantification. Hydrogeology Journal, 15(8): 1523-1534.
– IGRAC, 2017. Global Groundwater Information System (GGIS). IGRAC: International Groundwater Resources Assessment Center (https://www.un-igrac.org/global-groundwater-information-system-ggis), Netherland.
– Kowsar, S.A., 1991. Floodwater spreading for desertification control: an integrated approach. Desrtification Control Bulliten, 19: 3-18.
– Newman, J.C., 1963. Waterspreading on marginal arable areas. J. Soil Cons. NSW, 19: 49-58.
– Ouessar, M. et al., 2009. Modelling water-harvesting systems in the arid south of Tunisia using SWAT. Hydrol. Earth Syst. Sci., 13(10): 2003-2021.
– Pakparvar, M., 2015. Evaluation of floodwater spreading for groundwater recharge in Gareh Bygone Plain, southern Iran, Ghent University, Ghent, Belgium, 252 pp.
– Pakparvar, M. et al., 2014. Remote sensing estimation of actual evapotranspiration and crop coefficients for a multiple land use arid landscape of southern Iran with limited available data. J. of Hydroinformatics, 16(6): 1441-1460. DOI:http://dx.doi.org/10.2166/hydro.2014.140
– Pakparvar, M. et al., 20 .۱۸Artificial recharge efficiency assessment by soil water balance and modelling approaches in a multi-layered vadose zone in a dry region. Hydrological Sciences Journal: 1-20. DOI:10.1080/02626667.2018.1481962
– Philip, J.R., 1957. Theory of infiltration:-۱ The infiltration equation and its solution. Soil science, 83: 345–357.
– Quilty, J.A., 1972. Soil conservation structures for marginal arable areas diversion spreader banks and tank drains. J. Soil Con. N.S.W, 28: 157-168.
– Reynolds, W.D., Elrick, D.E., Youngs, E.G., 2002. Ring or Cylinder Infiltrometers (Vadose Zone). In: Dane, J.H., Topp, G.C. (Eds.), Methods of soil analysis, part4: Physical methods. SSSA Book Ser. 5. SSSA, Madison WI, pp. 818-826.
– Rushton, K.R., Ward, C., 1979. The estimation of groundwater recharge. 41: 345-361.
– Sanford, W., 2002. Recharge and groundwater models: an overview. Hydrogeol. J, 10: 110-120.
– Soil-Survey-Staff, 2010. Keys to Soil Taxonomy, . USDA-Natural Resources Conservation Service, Washington, DC.
– Soldevilla-Martinez, M., López-Urrea, R., Martínez-Molina, L., Quemada, M., Lizaso, J.I., 2013. Improving Simulation of Soil Water Balance Using Lysimeter Observations in a Semiarid Climate. Procedia Environmental Sciences, 19(0): 534-542. DOI:http://dx.doi.org/10.1016/j.proenv.2013.06.060
– Sophocleous, M.A., 1991. Combining the soilwater balance and water-level fluctuation methods to estimate natural groundwater recharge: practical aspects. Journal of Hydrology, 124(3): 229-241.
– Touhami, I. et al., 2013. Comparative performance of soil water balance models in computing semiarid aquifer recharge. Hydrological Sciences Journal, 59: 193-203. DOI:http://dx.doi.org/10.1080/02626667.2013.802094
– Wada, Y. et al., 2010. Global depletion of groundwater resources. Geophysical Research Letters, 37(20).
– Webb, R.M.T. et al., 2008. Variations in pesticide leaching related to land use, pesticide properties, and unsaturated zone thickness. J. Environ. Qual., 37: 1145–1157.